

Physical Optics Calculation of Electromagnetic Scattering from Haack Series Nose Cone

Z. Asadi and V. Mohtashami

Department of Electrical Engineering, Ferdowsi University of Mashhad, Mashhad, Iran,
z.asadi1990@gmail.com, v.mohtashami@um.ac.ir,
Corresponding author: V. Mohtashami

Abstract- In this paper, the physical optics method is used to study the problem of electromagnetic scattering from Haack series nose cone. First, a meshing scheme is introduced which approximates the curvature of the surface by piecewise linear functions in both axial and rotational directions. This results in planar quadrilateral patches and enables efficient determination of the illuminated region and application of closed-form expression for computing physical optics integral. Then the ray-surface intersections are obtained using the implicit surface equation of Haack series nose cone. The equation obtained by the intersection test does not have analytical solution. Hence, the Steffensen method is applied to solve this equation numerically. To find the initial point for Steffensen method's iterations, a bounding cylinder is used. It provides high precision evaluation of initial point, fast convergence and short computation time. Moreover, if the ray does not intersect the bounding volume, it certainly misses the bounded object and hence does not need to be tested in the Steffensen method. The ray-cylinder intersection test has a simple analytical solution, which results in fast rejection of missed rays. Simulation results demonstrate the proper accuracy and efficiency of the presented algorithms.

Index Terms- Bounding volume, Haack series, intersection test, mesh generation, physical optics.

I. INTRODUCTION

Physical Optics (PO) is a high frequency method that is widely applied to compute the scattering fields of electrically large objects [1]. It provides a good compromise between the accuracy of the simulation results and the computational cost [2], [3]. This method calculates the scattered field in two steps. The first step determines the illuminated region by the incident wave and the second step integrates the induced current over the illuminated portion of the surface to calculate the scattered field. For accurate determination of illuminated region and also PO integral calculation, the object should be represented by adequate number of meshes. Modeling the object with a large number of fine meshes increases the accuracy of geometric model at the cost of high computational burden

required for the identification of illuminated region. The computational performance of physical optics method is dominated by the meshing technique as well as the strategy used for finding illuminated meshes [4].

Choosing an appropriate meshing scheme depends on the geometric characteristics of the object. One of the important constituent parts of any vehicle or body which travels through a fluid medium is its nose cone. The determination of the nose cone geometrical shape plays a significant role in the aerodynamic design process of the object. Among the variety of commonly used nose cone shapes, Haack series provide the lowest theoretical wave drag and thus is aerodynamically desirable [5]-[7]. However, there is a very limited number of published papers in the area of electromagnetic scattering from Haack series nose cones [8], [9]. More work needs to be done to formulate and efficiently implement this geometry in scattering problems.

This paper is focused on the efficient and accurate implementation of Haack series nose cone for physical optics simulation of electromagnetic scattering. To efficiently determine the illuminated region and accurately calculate the physical optics integral, a mesh generation algorithm will be presented which approximates the curvature of the surface by piecewise linear functions [10]. As a result, the surface will be represented by a set of non-uniform quadrilateral patches. The use of quadrilateral patches instead of well known and often used triangular patches [11], enables finding the illuminated region of the surface through an efficient multilevel intersection test. Moreover, the patch vertices are coplanar. Hence, the physical optics surface integral is reduced to a closed form expression using Gordon's method [12]. In order to determine the illuminated patches, the ray-surface intersection test will be performed by substituting the ray equation into the implicit surface equation of Haack series. Then the obtained equation will be numerically solved using the iterative Steffensen's method. The initial point of Steffensen's iteration will be obtained by adopting the concept of bounding volumes. A bounding cylinder is used to speed up the rejection of missed rays and to efficiently find the initial point for iterative Steffensen's method.

The rest of this paper is organized as follows. Haack series equation, proposed meshing scheme and the formulation of ray-surface intersection test are presented in section II. Simulation results are provided in section III. Finally, conclusions are given in section IV.

II. PHYSICAL OPTICS SCATTERING FROM HAACK SERIES

A. Haack series

The Haack series nose cone is a body of revolution which is created by rotating its generatrix curve around an axis. The generatrix of Haack nose cone whose axis lies along the z-axis and its vertex lies at the origin is given by [13]

$$x = \frac{R}{\sqrt{\pi}} \sqrt{\theta - \frac{\sin 2\theta}{2} + C \sin^3 \theta} \quad (1)$$

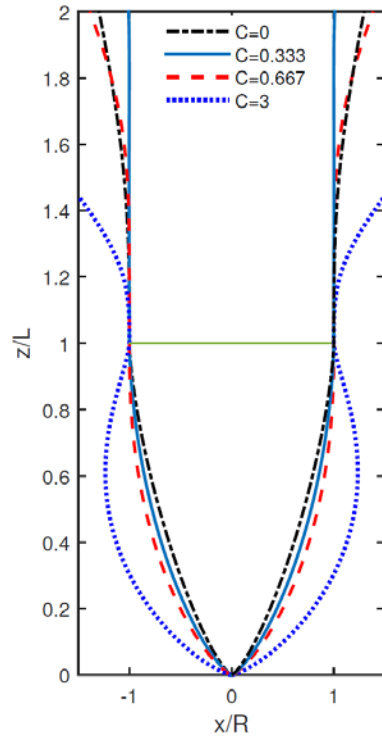


Fig. 1. Graphs illustrating Haack series shapes.

where

$$\theta = \cos^{-1}(1 - 2z/L) \quad (2)$$

In these equations R is the base radius, L is the length of nose cone and θ varies from 0, at the tip of nose cone, to π , at the base. The value of C determines the amount of nose curvature. Plots of the Haack series generatrix are depicted in Fig. 1 for sample values of C . For any value of C , $dx/dz|_{z=L} = 0$. Therefore, the base of the nose cone will always be tangent to the cylindrical fuselage of the missile/aircraft and eliminates the diffraction of incident wave. Two values of C have practical importance in the design of flying military objects. When $C = 0$, the Haack series nose cone achieves minimum drag for a given length and radius [13]. This shape is usually referred to as LD-Haack or the Von Karman. When $C = 1/3$, the Haack series nose cone is referred to as LV-Haack and achieves minimum drag for a given length and volume of nose cone [13]. For $C > 2/3$ Haack series shape bulges out to a maximum diameter that is greater than the base diameter as shown in Fig. 1 for $C = 3$. This case, however, is seldom used due to aerodynamic considerations.

B. Meshing Scheme

The efficiency of PO-based scattering calculations, depends primarily on the meshing scheme used for modeling the object surface. The meshing algorithm has to be chosen such that 1) the part of the



Fig. 2. The meshing scheme for bodies of revolution.

surface illuminated by the incident wave is determined efficiently, and 2) the physical optics scattering integral is calculated efficiently. Traditionally, the surface of the object is described by a mesh network of triangular planar patches [11] because the intersection test with planar surfaces can be solved analytically. The brute-force ray tracing is therefore applied to test each launched ray against all patches [14]. For large and geometrically complex objects with a large number of patches, the brute-force ray tracing is supplemented by acceleration techniques such as kd-tree [15] and space division [16] to reduce the computational burden. The utilization of triangular flat patches enables closed-form calculation of the physical optics scattering integral by using Gordon's method [12] and, hence, reducing computational burden.

The meshing scheme for bodies of revolution can be modified to reduce the number of patches and improve the efficiency of the simulation. In [10], quadrilateral patches have been used to model the geometries with axial symmetry as shown in Fig 2. In this methodology, the object surface is approximated along φ and z directions by piecewise linear functions. The approximation is performed uniformly along φ whereas the number and lengths of line segments along z are determined adaptively. These approximations are done so as to minimize the phase error of incident ray that hit the approximate function [10]. By choosing proper tessellation frequencies along φ and z directions, the curvature of the object is properly included.

Since Haack series is a body of revolution with axial symmetry, the mentioned process is applicable for meshing its surface. In this process, (1) is incorporated as the generatrix of the Haack series. The resulting quadrilateral patches are planar due to uniform tessellation along φ . To determine the illuminated patches, each ray is tested against the surface by inserting the parametric ray equation into the explicit surface equation. This yields a one variable algebraic equation whose solution is used in the ray equation to determine the intersection point. The PO scattering integral is still efficiently calculated by the Gordon's method due to the planar shape of the patches. In this

approach, the main challenges are efficiently solving this one-variable equation as well as finding the patch that circumscribes the intersection point. The latter challenge is properly addressed by the incorporated meshing scheme; the φ and z coordinates of the intersection point are described in local coordinates of the Haack series and the circumscribing patch is easily found. The former challenge, however, is more complicated which is addressed in more details in the following subsection.

C. Formulation of Intersection Test

The position vector of a ray launched from the point $R_0 = (x_0, y_0, z_0)$ which propagates along the direction $\hat{s} = s_x \hat{x} + s_y \hat{y} + s_z \hat{z}$ is defined by the parametric equation $\bar{R}(t) = \bar{R}_0 + \hat{s}t$. In this equation t is the parameter which equals the distance from the ray's origin. Substituting the ray equation into the Haack series surface equation yields the following quadratic equation

$$h(t) = p_2 t^2 + 2p_1 t + p_0 - \frac{R^2}{\pi} \left[\cos^{-1}(1 - 2z/L) - \frac{1}{2} \sin(2 \cos^{-1}(1 - 2z/L)) + C \sin^3(\cos^{-1}(1 - 2z/L)) \right] = 0 \quad (3)$$

where $p_2 = s_x^2 + s_y^2$, $p_1 = x_0 s_x + y_0 s_y$, $p_0 = x_0^2 + y_0^2$, and $z = s_z t + z_0$. The insertion of the smaller positive solution t gives the intersection point. This process is repeated for every ray cast from the ray source. Hence, improving the performance of each intersection test is very important. Note that (3) has no analytical solution and iterative numerical methods have to be used to solve it. Newton-Raphson method and Steffensen method are considered as good candidates for this purpose and formulated as

$$t_{n+1} = t_n - \frac{h(t_n)}{g(t_n)} \quad (4)$$

where $g(t_n) = h'(t_n)$ in Newton-Raphson method, and $g(t_n) = (h(t_n + h(t_n)) - h(t_n)) / h(t_n)$ in Steffensen method [17]. While its function evaluations and order of convergence are the same as Newton-Raphson method, the Steffensen method avoids using function derivative and hence is more robust near the function's stationary points. Both methods yield quadratic convergence to the result provided that a good initial value for t is used [17].

A suitable approach for finding the initial value of t is using the concept of bounding volumes which is widely used in computer graphics and site-specific propagation modeling [18]. The bounding volume is a simple geometric object, such as planar box, cylinder or sphere. It surrounds the original object and its intersection test is numerically simple to solve. Initially, the intersection test is performed against bounding volume. If the ray misses the bounding volume, it certainly does not hit

the original object and is discarded. If the ray hits the bounding volume, it may hit the original object and has to be checked against it. For this strategy to be effective, the overall shape of the bounding

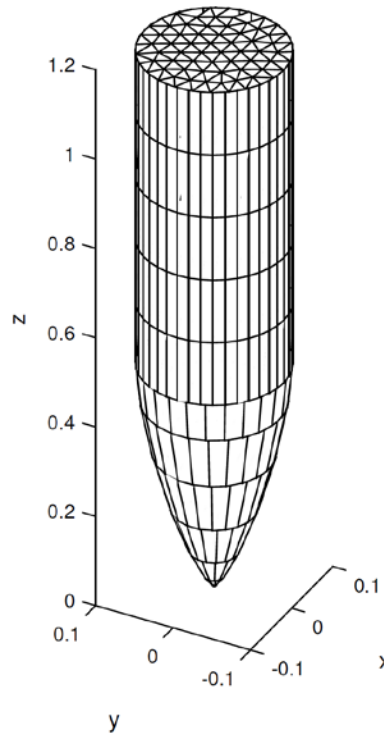


Fig. 3. Geometry of simple generic missile.

volume should be similar to the original object in order to minimize the number of rays that hit the bounding volume but miss the original object. For the Haack series nose cone, cylindrical bounding volume seems to be a suitable choice. This guess is confirmed in the numerical results.

The value of t found from checking the ray against the bounding volume is used as the initial value of the iterative Newton-Raphson or Steffensen method. The iterations are repeated until either (a) the convergence occurs, or (b) a maximum number of iterations is reached. The threshold for convergence check depends on mesh resolution. Under case (a), the value of t is inserted into the ray equation and the intersection point is calculated. It should be noted that the intersection point is valid only if its z coordinate lies within the length of nose cone. Then the quadrilateral mesh that circumscribes the intersection point is found by considering the φ and z coordinates of the intersection point as described in section II-B. If the iterations are terminated by case (b), the algorithm does not find any solution and ray does not hit the nose cone.

III. SIMULATION RESULTS AND DISCUSSION

For verification of the proposed algorithms, scattering from a simple missile model is studied. The geometry of the missile is shown in Fig. 3. The nose cone is of LD-Haack shape which has a length of

0.5 m and a base radius of 0.09 m, and the overall length of the missile is 1.2 m. For meshing the surface, the nose and the fuselage are modeled by quadrilateral patches according to the methodology

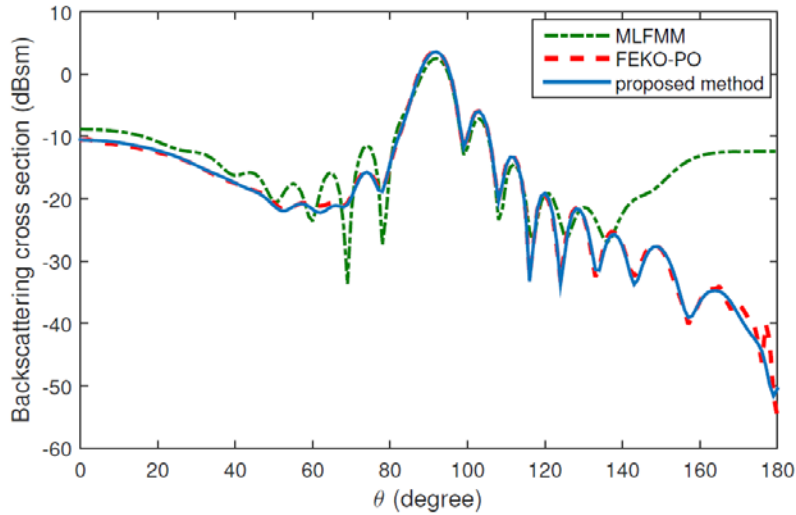


Fig. 4. Backscattering cross section pattern for simple missile model in Fig.3.

described in section II-B. The surface of backend disk is meshed by the popular Delaunay Triangulation method [19]. A total number of 439 quadrilateral and triangular patches are used to represent the missile model depicted in Fig. 3.

Prior to studying the efficiency of the proposed meshing scheme and intersection test algorithm, it is essential to validate the PO code used in the simulations. The backscattering radar cross section of the missile is studied in the yz plane for incident angles $\theta = 0^\circ$ to $\theta = 180^\circ$ at $f = 1$ GHz with an angular resolution of 1° and vertical polarization. The obtained PO results are compared with the Multi-Level Fast Multipole Method (MLFMM) as the reference solution in Fig. 4. As observed, the result of our PO code agrees well with that of MLFMM. The discrepancies are associated with faceting errors of the curved surface as well as unconsidered scattering mechanisms in PO code such as edge diffraction and creeping waves. For the sake of comparison, the PO simulation of the commercial FEKO software is also included in Fig. 4. As observed, our PO results agree very well with PO analysis of FEKO. Table I summarizes the runtime performance and memory consumption of different methods. The computation time is the total simulation time for all incident angles. The computer used in all simulations has an Intel Core i5-42000 CPU @ 1.60 GHz, 2.30 GHz processor and 6 GB of RAM.

To efficiently implement the proposed intersection test algorithm for nose cone, a suitable bounding volume should be chosen. Two candidates are studied, a sphere and a cylinder. The intersection test with both of these shapes result in a quadratic equation with an analytical solution. Hence, very little computational burden is imposed. The sphere has a diameter of $D_s = L + R^2/L$ and

its center is located at $(0,0,D_s/2)$. This is the smallest enclosing sphere of a Haack series nose cone. The bounding cylinder and the nose cone are coaxial and have the same diameter. In this case, if the incident ray does not intersect the cylinder, it is tested against the frontal circular face. The intersection parameter t with the bounding volume is passed to the iterative Steffensen method as the

Table I. Comparison of the computation time and memory consumption of three different methods for geometry in Fig. 3.

| Method | Computation time | Memory consumption |
|-----------------|------------------|--------------------|
| Proposed method | 14.3 sec | 0.157 MB |
| PO-FEKO | 17 sec | 2.2 MB |
| MLFMM-FEKO | 5 min | 2.9 MB |

Table II. Comparison of the computation time for two different bounding volumes

| Bounding volume | Computation time (sec) |
|-----------------|------------------------|
| Cylinder | 3.5 |
| Sphere | 5.1 |

Table III. Comparison of the efficiency of the iterative numerical methods

| Numerical method | Computation time (sec) |
|------------------|------------------------|
| Steffensen | 3.7 |
| Newton-Raphson | 3.8 |

Table IV. The computation time of the proposed method compared with brute-force ray tracing

| Method | Computation time (sec) |
|---|------------------------|
| Proposed method | 14.3 |
| Brute-force ray-patch intersection test | 43 |

Table V. Comparison of the computation time and memory consumption of three different methods for geometry in Fig. 5.

| Method | Computation time | Memory consumption |
|-----------------|------------------|--------------------|
| Proposed method | 1.5 min | 1.5 MB |
| PO-FEKO | 1.5 min | 3.7 MB |
| MLFMM-FEKO | 25 hours | 6.5 MB |

initial value. In Table II, the overall runtime performance of these two cases are reported which demonstrates the supremacy of the cylindrical bounding volume. The reason is that the volume of the bounding sphere is more than the volume of the bounding cylinder. In other words, the bounding cylinder fits better to the nose cone. Hence, if a ray hits the bounding cylinder, it is more likely to hit the nose cone.

The next step is to choose a good iterative technique to solve the ray-Haack intersection test. As stated in section II-C, Steffensen and Newton-Raphson methods are good candidates with quadratic order of convergence. To choose among these two candidates, intersection tests are performed for the nose cone and the run-time performance is evaluated. In both cases, the cylindrical bounding volume is used to determine the initial value of the iterations. The simulation time of the intersection test

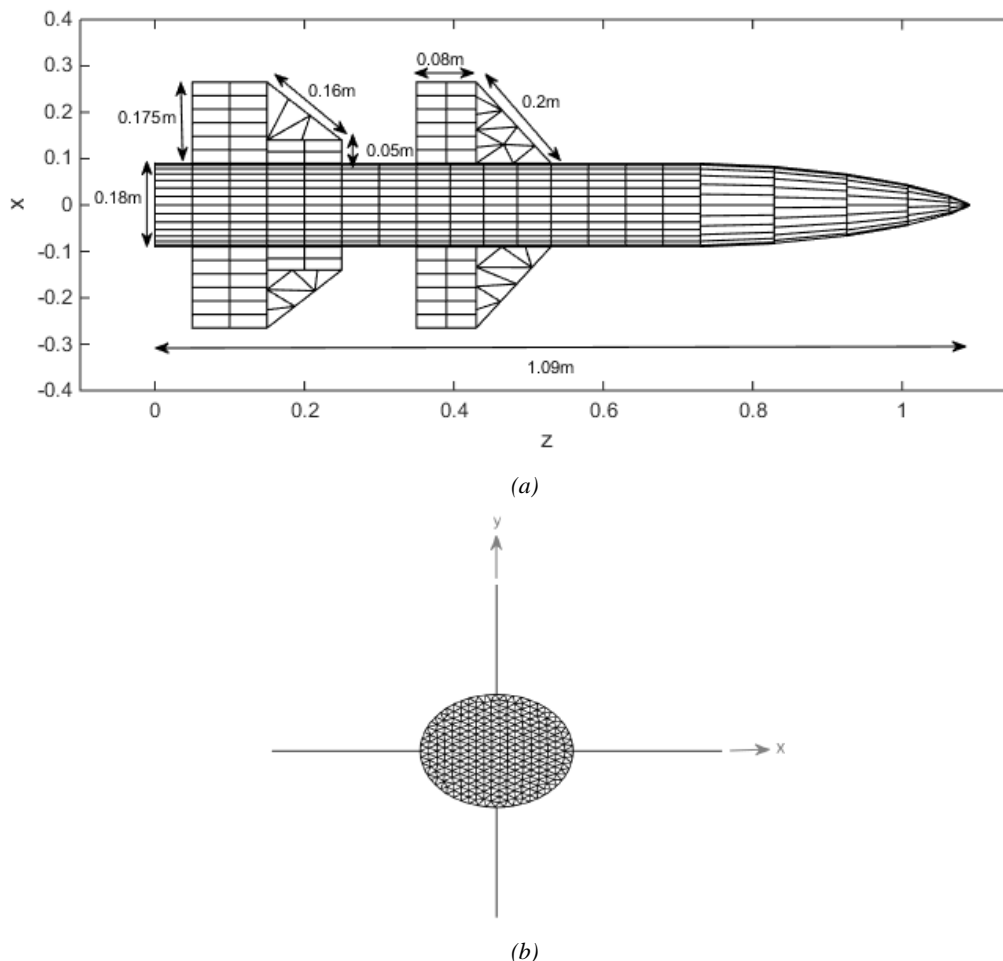


Fig. 5. Geometry of realistic missile model, (a) lateral view (b) back view.

algorithms are presented in Table III. As observed, the Steffensen method is slightly superior which is associated with the absence of the function derivative in its formulation.

Finally, the computational efficiency of our proposed strategy is assessed by comparing its simulation time with brute-force ray tracing. To do this, two situations are considered for calculating the backscattering cross section of geometry depicted in Fig. 3. First, the illuminated patches are determined using our proposed multilevel procedure described in section II. In this case, the intersection points are calculated by using the cylindrical bounding volume and Steffensen method. Second, the brute-force ray tracing is performed to find the intersected patches. In this case, each launched ray is tested, in parallel, against the planar quadrilateral and triangular patches and the intersected patch is determined. In both simulations, the Gordon's method [12] is used for calculating

the scattering contribution of illuminated patches. In Table IV, runtime performances for these two methods are reported. The simulation results indicate that a speedup of about three times is obtained by using proposed algorithm.

To further verify the accuracy and efficiency of proposed method, a realistic missile model is simulated to compare the results of presented method with MLFMM as well as PO simulation of

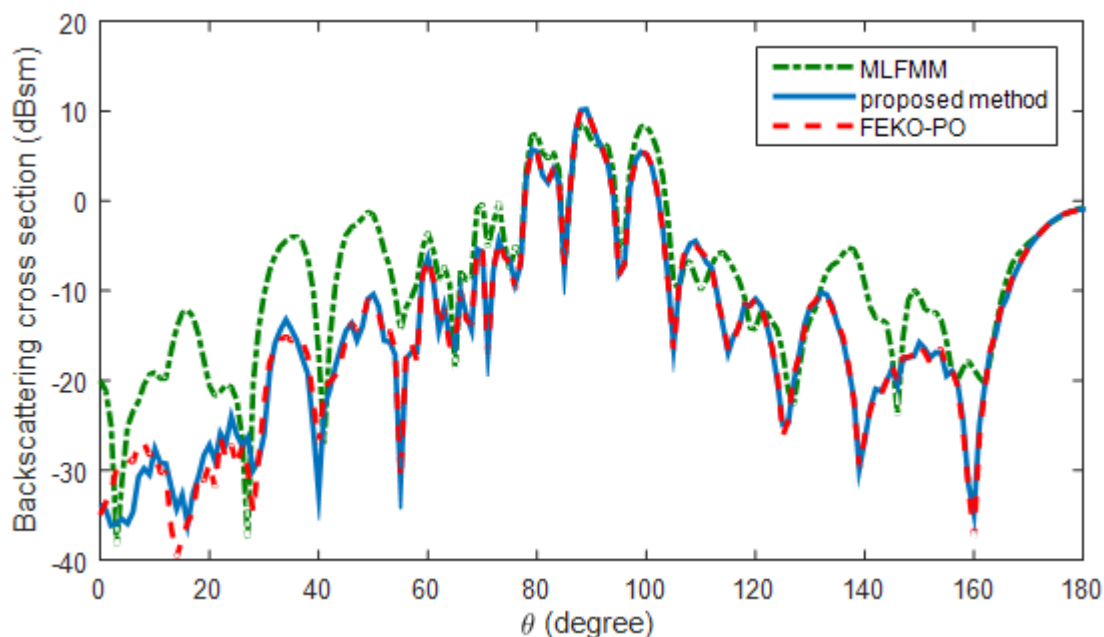


Fig. 6. Backscattering cross section pattern for realistic missile model in Fig.5.

FEKO. The geometry of this target is shown in Fig. 5. The nose cone is a LV-Haack with a length of 0.36m and a base radius of 0.09m. In this case, the frequency is set to 3 GHz and the backscattering cross section for vertical polarization is calculated in the yz plane for incident angles $\theta = 0$ to $\theta = 180$ with an angular resolution of 1° . Fig. 6 shows the simulation results. Perfect agreement is observed between the results of the proposed method and the PO simulations of FEKO. The discrepancies between the PO simulations and the MLFMM are attributed to the errors caused by the faceting of the curved surface and ignoring the edge and tip diffraction effects. The computation time and also memory usage for these three simulations are compared in Table V. The results show that the efficiency and accuracy of proposed method and PO simulation of FEKO are of the same order. It should be noted that FEKO is a leading electromagnetic software which uses various acceleration techniques both in ray tracing and calculating of physical optics integral. The proposed method is done without using acceleration techniques. Therefore, the proposed algorithm is able to achieve a much better performance in PO calculation for Haack series nose cones when supplemented by proper ray tracing acceleration techniques.

IV. CONCLUSION

A technique has been presented in this paper for efficient calculation of electromagnetic scattering from Haack series nose cone based on the physical optics method. In the proposed technique, an efficient meshing algorithm is used which expresses the surface of the object in terms of quadrilateral planar patches. This algorithm improves the performance of intersection test and simplifies the calculation of the physical optics integral. The ray-surface intersection test is performed by using the implicit surface equation of Haack series. This results in an algebraic equation which is solved by using the iterative Steffensen method. A bounding cylinder is used to provide an appropriate initial point for the Steffensen method. After finding the intersection point, the enclosing patch is efficiently found via a multilevel procedure based on the applied meshing algorithm.

The simulation results show that the efficiency of illuminated region identification is significantly improved. A speedup of about 3 times is obtained compared to the brute-force ray-patch intersection test. The closed-form calculation of the radiation integral also improves the efficiency while retaining the accuracy. The simulation results show that the backscattering cross section prediction for the Haack series nose cone has a good agreement with MLFMM simulation.

REFERENCES

- [1] C. A. Balanis, *Advanced Engineering Electromagnetics*. Wiley, 1989.
- [2] C. Uluisik, G. Cakir, M. Cakir, and L. Sevgi, "Radar cross section (RCS) modeling and simulation, part 1: a tutorial review of definitions, strategies, and canonical examples," *Antennas and Propagation Magazine, IEEE*, vol. 50, no. 1, pp. 115–126, Feb 2008.
- [3] F. Weinmann, "Ray tracing with PO/PTD for RCS modeling of large complex objects," *IEEE Transactions on Antennas and Propagation*, vol. 54, no. 6, pp. 1797–1806, June 2006.
- [4] F. S. Adana, *Practical applications of asymptotic techniques in electromagnetics*. Artech House, 2010.
- [5] M. Choudhari, N. Tokugawa, F. Li, C. Chang, J. White, H. Ishikawa, Y. Ueda, T. Atobe, and K. Fujii, "Computational investigation of supersonic boundary layer transition over canonical fuselage nose configurations," *Seventh International Conference on Computational Fluid Dynamics (ICCFD7)*, Big Island, Hawaii, 2012.
- [6] R. Harris and E. Landrum, "Drag characteristics of a series of low-drag bodies of revolution at mach numbers from 0.6 to 4.0," *National Aeronautics and space administration, NASA TN D-3163*, 1965.
- [7] T. von Karman, *Aerodynamics*. Literary Licensing, LLC, 2013.
- [8] E. Arvas and S. Ponnappalli, "Scattering cross section of a small radome of arbitrary shape," *IEEE Transactions on Antennas and Propagation*, vol. 37, no. 5, pp. 655–658, May 1989.
- [9] P. L. Overfelt, "Superspheroids: a new family of radome shapes," *IEEE Transactions on Antennas and Propagation*, vol. 43, no. 2, pp. 215–220, Feb 1995.
- [10] Z. Asadi and V. Mohtashami, "Efficient meshing scheme for bodies of revolution-application to physical optics prediction of electromagnetic scattering," *Progress in Electromagnetics Research M*, vol. 48, pp. 163–172, 2016.
- [11] N. Youssef, "Radar cross section of complex targets," *Proceedings of the IEEE*, vol. 77, no. 5, pp. 722–734, May 1989.
- [12] W. Gordon, "Far-field approximations to the Kirchoff-Helmholtz representations of scattered fields," *IEEE Transactions on Antennas and Propagation*, vol. 23, no. 4, pp. 590–592, Jul 1975.

- [13] W. Stoney, "Transonic drag measurements of eight body-nose shapes," *National Advisory Committee for Aeronautics*, 1957.
- [14] J. Havel and A. Herout, "Yet faster ray-triangle intersection (using SSE4)," *IEEE Transactions on Visualization and Computer Graphics*, vol. 16, no. 3, pp. 434–438, May 2010.
- [15] Y.-B. Tao, H. Lin, and H.-J. Bao, "Kd-tree based fast ray tracing for RCS prediction," *Progress in Electromagnetics Research*, vol. 81, pp. 329–341, 2008.
- [16] K.-S. Jin, T.-I. Suh, S.-H. Suk, B.-C. Kim, and H. T. Kim, "Fast ray tracing using a space-division algorithm for RCS prediction," *J. Electromagn. Waves Appl.*, vol. 20, no. 1, pp. 119–126, 2006.
- [17] G. Dahlquist and A. Bjorck, *Numerical Methods in Scientific Computing: Volume 1*. Philadelphia, PA, USA: Society for Industrial and Applied Mathematics, 2008.
- [18] A. S. Glassner, *An introduction to ray tracing*. Academic press, 1989.
- [19] P.-O. Persson and G. Strang, "A simple mesh generator in MATLAB," *SIAM Review*, vol. 46, no. 2, pp. 329–345, June 2004.